OPTOELECTRONICS AND ADVANCED MATERIALS – RAPID COMMUNICATIONS Vol. 6, No. 5-6, May - June 2012, p. 618 - 622

Excellent insulating behavior Al_2O_3 thin films grown by atomic layer deposition efficiently at room temperature

YUDE SHEN[a], YAWEI LI[a], JINZHONG ZHANG[a], XIA ZHU[a], ZHIGAO HU[a], JUNHAO CHU[a,b]
[a]*Key Laboratory for Polar Materials and Devices of Ministry of Education, East China Normal University, Shanghai, 200241, People's Republic of China*
[b]*National Laboratory for Infrared Physics, Shanghai Institute of Technical Physics, Chinese Academy of Sciences, Shanghai, 200083, People's Republic of China*

Al_2O_3 thin films were deposited at room temperature by atomic layer deposition (ALD) method with trimethylaluminum and ozone. The deposition velocity can be improved two orders of magnitude with the using of O_3 instead of H_2O. The Al_2O_3 films surface are atomically smooth. It was found that there are much less defects density in the O_3-based Al_2O_3 film than H_2O-based one. The O_3-based Al_2O_3 film shows excellent insulating behavior and the breakdown field is about 7 MV/cm. These results prove the superior quality of the O_3-based film, which is suitable for microelectronic devices.

(Received April 7, 2012; accepted June 6, 2012)

Keywords: Al_2O_3 thin films, Atomic layer deposition, Insulating behavior, Breakdown field

1. Introduction

Al_2O_3 attracts much interest because of its unique properties, such as wide band gap (~9 eV), high breakdown electric field (5-10MV/cm), high permittivity, excellent dielectric properties, strong adhesion to various materials, high thermal and chemical stabilities, which make it widely used as insulating material for gate dielectric, tunneling barrier, and protective coating [1-3]. Compared to the conventional process, i.e., sputtering, electron-beam evaporation, chemical vapor deposition, or oxidation of pure Al films, the Al_2O_3 film deposited by Atomic layer deposition (ALD) method has a much higher quality [4]. ALD has become an effective solution for preparation of thin films because of its precise control in the film thickness and composition with excellent uniformity, and near perfect conformal step coverage. In general, under proper ALD conditions the growth rate per cycle (GPC) is constant and independent of process parameters (e.g., temperature, pressure and flow rate). The corresponding temperature range is the so-called ALD window. The self-limiting growth mechanism facilitates the growth of a film with thickness control on atomic scale on large areas. Al_2O_3 coatings prepared by ALD on organic can be used as gas diffusion barriers or passive layer for flexible electronic devices, organic light emitting diodes (OLEDs), and dye-sensitised solar cells (DSSCs)[5-8]. However, desired properties of Al_2O_3 films have been found to be optimized in excess of a ALD growth temperature of 350 °C[9-11]. Such high temperature would degrade organic, polymeric, and biological materials. It is necessary to explore the low-temperature ALD process of Al_2O_3.

Using of catalyst or employing of plasma-enhanced ALD (PE-ALD) can reduce the deposition temperature [12, 13]. However, catalyst often introduces foreign impurities. For example, nitrogen impurities occurred in the SiO_2 film that deposited using $SiCl_4$ and H_2O with an NH_3 catalyst [12]. The using of PE-ALD will result in more difficult process control, limited 3-dimensional coating capability, and the equipment becomes more complex and expensive [14]. For example, Kääriäinen *et al.* prepared Al_2O_3 films by PE-ALD with trimethylaluminum (TMA) and O_2 [15]. In their process, the by-product H_2O produced by the plasma led to additional chemical vapor deposition (CVD) type growth of Al_2O_3, and the GPC of the Al_2O_3 films was dependent on the growth conditions (such as the plasma power, O_2 plasma pulse length and the distance between plasma source and substrate). Additionally, significant nitrogen impurities in the film were observed [15]. All these drawbacks weaken the advantage of ALD process. An exploration for the deposition of Al_2O_3 films at lower temperature with a conventional ALD process had been reported by Groner *et al* [16]. They accomplished the Al_2O_3 with TMA and H_2O reactants at temperatures as low as 33 °C without the use of any catalyst. Because of the large dipole momentum of H_2O molecule, H_2O has a high surface affinity, slow desorption rate of H_2O at low temperature requires extremely longer purge times to avoid the CVD-type growth [16]. Additionally, the breakdown field is only 3.7 MV/cm for the Al_2O_3 films due to the excessive hydrogen purities. The extremely low growth velocity and low breakdown field limit its applications.

In this letter, we report the growth of Al_2O_3 films by ALD method at room temperature (RT), O_3 instead of H_2O was employed as oxygen precursor. This study explored the growth parameters for low-temperature deposition of Al_2O_3 films and examined the properties of the resulting films. The growth velocity greatly increased due to the using of O_3 instead of H_2O. The excellent insulating behavior of the O_3-based films was observed.

2. Experiment

The Al_2O_3 films were synthesized on silicon substrates via ALD (Sunale R-75, Picosun Oy.). TMA and ozone were employed as aluminum and oxygen sources, respectively. High purity nitrogen (99.9995%) was used as the carrier and purging gas. Prior to deposition, the Si(100) substrates were pre-cleaned by de-ionized water and alcohol and dried with pure nitrogen flow. During the deposition process, the reaction chamber was kept at room temperature (RT). TMA and ozone was alternately introduced into the reaction chamber with N_2, and N_2 purge flow was inserted between the two precursors pulse. The carrier and purging gas flow rate for both TMA and O_3 were 150 sccm (standard cubic centimeters per minute). The O_3 flow was fixed as 250 sccm and pulse 3s, purge 6s based on our previous study. For comparison of the electrical properties of the O_3-based and H_2O-based Al_2O_3 films, H_2O was also employed as oxygen source to synthesize Al_2O_3 films at room temperature and 300 ^{o}C, respectively. The corresponding H_2O purge times were 8 s and 4 s, respectively. In all deposition processes, the pulse time of TMA and H_2O were 0.1s.

The thicknesses of Al_2O_3 films were measured by spectroscopic ellipsometry (SE). The morphology of the samples was observed by a field emission scanning electron microscope (FE-SEM, Philips XL30FEG) and an atomic force microscope (AFM; Dimension 3100). The topper Al electrodes were fabricated via thermal evaporation through a shadow mask. The dielectric properties of the Al/Al_2O_3/Pt metal-insulator-metal (MIM) capacitors and capacitance-voltage (C-V) measurement for Al/Al_2O_3/n-Si metal-insulator-semiconductor (MIS) structure were measured using a dielectric analyzer (BDS40, Novocontrol Tech.). The sweep rate of voltage for the C-V measurement is about 0.1V/s, and the voltage dependence of capacitance is recorded with a 1MHz small ac signal of 50mV. The leakage current and breakdown electric field of Al_2O_3 films were measured by an electrometer (Kethley 6517A).

3. Results and discussions

The topographic information of the Al_2O_3 films was studied. The O_3-based Al_2O_3 film exhibited excellent smoothness, as shown in Fig. 1(a). While the H_2O-based Al_2O_3 film was rather rough and abundant particles presented, as shown in Fig. 1(b). It may due to that the residual H_2O reacts with the precursors and form small particles [17]. The root mean square (RMS) of the O_3-based as-deposited films (TMA purge time 2 s,1000 ALD cycles) is 0.245 nm over a scanned area of 0.5 × 0.5 μm^2 measured by AFM, and it approximates to that of Si substrate. The samples with different film thickness all possess such atomically smooth surface. It implies that the growth possibly follows 2D layer-by-layer growth mode.

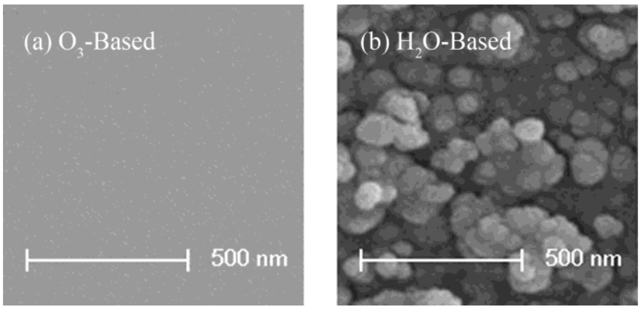

Fig. 1. The SEM images of (a) O_3-based and (b) H_2O-based Al_2O_3 films deposited at room temperature. Note that the purge times after TMA exposure were 2 s and 8 s for the O_3-based and H_2O-based films, respectively.

The pulse time of TMA was fixed as 0.1s. It is sufficient to ensure the surface of substrate be fully covered with TMA [18]. Fig. 2(a) shows the effect of TMA purge times on the GPC at room temperature. The GPC (about 1.25 Å/cycle) is almost independent of TMA purge time range from 2 to 12s. This indicates that excessive TMA can be very easily purged, and the minimum of the purge time 2 s is long enough to eliminate multilayer adsorption and prevent subsequent CVD-type growth. In the TMA/H_2O process, the GPC of Al_2O_3 film decreased with the purge time of H_2O increased, only if extremely long time was chosen, the GPC approached a constant value [16]. In our studies, effect of shorter TMA purge time on GPC was not investigated because of the requirement for complete separation of the TMA/O_3 pulse. Therefore, the declining segment of the curve like the TMA/H_2O process can not be observed. The film thickness as function of deposition cycles was investigated. Figure 2(b) reveals the thickness of films as a function of the number of ALD cycles. The linearity indicates that the thickness of Al_2O_3 films can be precisely controlled by the number of ALD cycles.

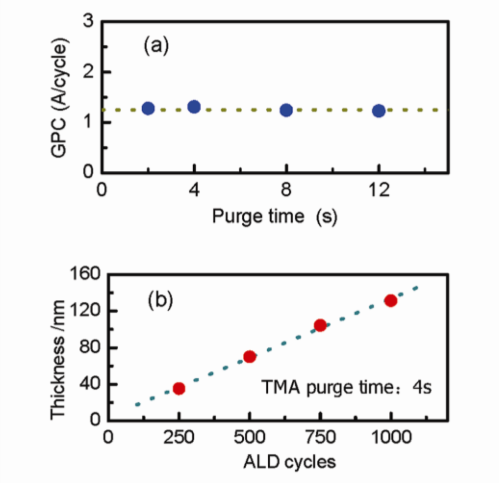

Fig. 2. (a) The dependence of the O_3-based Al_2O_3 growth rate on the purge time at room temperature. (b) Al_2O_3 films thickness versus number of ALD cycles at room temperature with the purge time 4s.

It is well known that monolayer forms on the surface of substrate per cycle in the ALD window [19]. The condensation will occur at low temperature and multilayer forms due to physisorption, which may result in the uncontrollable growth [19]. A deliberately chosen long purge time may transfer multilayer adsorption to monolayer adsorption, and the ALD process may realize at lower temperature, which had accomplished by Groner *et. al* [16]. Both in TMA/H_2O and TMA/O_3 ALD process, the high volatility of TMA ensures the short purge time for TMA. On the other hand, in low temperature TMA/H_2O ALD process, it is very difficult to purge H_2O because of its high surface affinity. Although the extremely long purge time for H_2O can realize the ALD process and lead to the smoothness of the Al_2O_3 films, the minimum purge times reached 180 s at 33 ^{o}C to realize the true ALD growth [16]. The extremely low deposition velocity is insufferable. As a gas oxygen source, ozone can be purged more efficiently than water and does not require a special surface preparation. The purge time reduced two orders of magnitude due to the using of O_3 instead of H_2O in our studies. Therefore, the amelioration of the process can greatly improve the throughput and provide more flexibility [20, 21].

The investigation of electrical properties of the Al_2O_3 films deposited at low temperature by PE-ALD was absent [15]. Herein, we compared the electrical properties of O_3-based film with H_2O-based film deposited at room temperature. The C-V measurements were performed on the low-temperature as-deposited Al_2O_3 ALD films. The C-V curve for O_3-base Al_2O_3 shows a saturation behavior in the accumulation region due to the low leakage current [22]. as shown in Fig. 3(a). The shift of flatband voltage [23] (ΔV_{FB}) for the O_3-base Al_2O_3 is about 0.02V, which is even less than that (0.196V) of the H_2O-based Al_2O_3 films deposited at 350 ^{o}C [9]. While a rather lager ΔV_{FB} (2.25V) for the H_2O-base Al_2O_3 deposited at room temperature can be observed, as shown in Fig. 3(b). The defects like unoxidized Al or -OH radicals may result in the lager ΔV_{FB} for H_2O-base Al_2O_3 film [16, 24] The Al-Al bond was observed in the case of TMA/H_2O ALD process with *n*-Si substrate [16, 24] At lower temperatures, the H_2O in TMA/H_2O ALD process can remain on the surface, and the hydroxyl surface coverage on Al_2O_3 surfaces is higher [25]. In addition, the reaction of TMA with the Al-OH surface species groups is not complete at low temperatures [25]. The window of C-V for H_2O-based MIS capacitor may due to the -OH radicals. It is well known that the hysteresis voltage (ΔV_{FB}) of the C–V curve can be used to estimate the “slow” interfacial state density (N_{si}) using the following equation [26]:

$$N_{\mathrm{si}} = \frac{C_{ox}\Delta V_{\mathrm{FB}}}{qS} \qquad (1)$$

Where C_{ox} is the capacitance of the oxide layer, q is the electron charge; S is the area of capacitance. The N_{si} of H_2O-based sample was estimated to be 1.9 × 10^{12} cm^{-2}, which is much higher than that of the O_3-based sample (about 4.2 × 10^{10} cm^{-2}). The -OH radical acts as an impurity at the interface and degrades the quality of the Al_2O_3 films, and using of O_3 is helpful to prevent the formation of -OH radical [23]. On the other hand, in TMA/O_3 ALD process, O_3 acts as an active oxidant and the following reaction takes place [24]:

$$2Al(CH_3)_3+O_3 \rightarrow Al_2O_3+3C_2H_6 \qquad (2)$$

It implies that using of O_3 for the Al_2O_3 film can suppress the presence of -OH radicals compares to H_2O-based process; the by-product ethane can be efficiently purged. Therefore, much lower defects density in the O_3-based films facilitates the improvement of the insulating behavior and C-V characteristics.

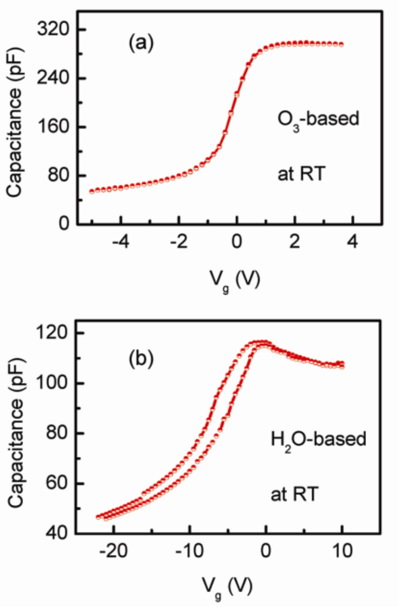

Fig. 3. The C-V characteristics of Al/Al_2O_3/n-Si MIS capacitors were measured at 1MHz. (a) O_3-based and (b) H_2O-based Al_2O_3 were deposited at room temperature by ALD with 1000 cycles.

The capacitance-frequency (C-F) measurements were performed to investigate the dielectric property of the O_3-based Al_2O_3 films. The dielectric constant is independent of frequency in the range of 10^2 - 10^6 Hz, as shown in Fig. 4. The excellent dielectric properties of Al_2O_3 film prepared at room temperature may well be utilized as capacitor dielectrics.

The inset of Fig. 4 shows the dependence of capacitance on the Al_2O_3 thickness at 100 kHz. The good linearity confirms that the thickness of Al_2O_3 films can be precisely controlled by number of ALD cycles. The 1/C axis offset in the relative cycles is about 4.8×10^{-4} pF^{-1}. It may attribute to an interfacial layer. Therefore, the overall measured capacitance (C_{total}) can be expressed by

$$\frac{1}{C_{total}} = \frac{1}{C_{\mathrm{i}}} + \frac{d_x}{\varepsilon_o \varepsilon_r S} \tag{3}$$

Where C_i is the capacitance of interfacial layer, d_{x} is the thickness of Al_2O_3 film, ε_0 is the vacuum permittivity, ε_r is the relative dielectric constant of the Al_2O_3 film, S is the area of the electrode. The dielectric constant ε_r can be calculated from the slope of line and the value is about 8, which is identical to that of H_2O-based Al_2O_3 films (~8) deposited at 350 ^oC [10].

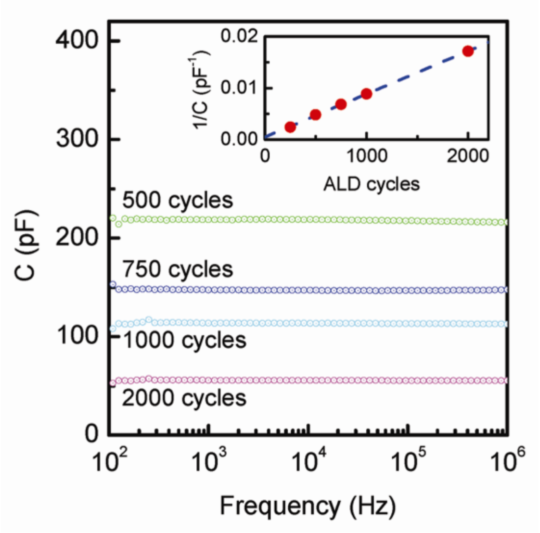

Fig. 4. The C-F characteristics of different thickness Al_2O_3 capacitors. The inset shows the dependence of capacitance on ALD cycles at 100 KHz.

We also compared the leakage of O_3-based Al_2O_3 film (deposited at room temperature) with the H_2O-based Al_2O_3 film (deposited at 300 ^oC). Fig. 5 shows the current density vs. electric field (J-E) plots of them. The two kinds of films show different leakage behaviors. According to the post-breakdown resistance, the breakdown events for H_2O-based and O_3-based films can be regarded as “soft” breakdown and “hard” breakdown, respectively [27]. For the H_2O-based film, the rise of current from approximately 4 MV/cm can be identified as Fowler–Nordheim (FN) tunneling [28], as shown in the inset of Figure 5. The rising segment in the range of 5.8 to 7MV/cm may attribute to the dissociation of -OH radicals at a higher electrical field [29]. The O_3-based film demonstrates a very low leakage current density, and the excellent insulating behavior of films (before catastrophic breakdown) corresponds to resistivity higher than 10^{17} Ω·cm. It has a higher breakdown field (E_{bd}) of about 7 MV/cm compare to that of H_2O-based Al_2O_3 film (3.7 MV/cm) [16]. For the O_3-based film, no any noticeable gradual rising present even though the minimum voltage step (0.005V for Kethley 6517A) was chosen. The leakage current increased 7-8 orders of magnitude suddenly and damaged the film and electrode. It implies that the O_3-based Al_2O_3 film has an excellent insulating performance, and the breakdown occurred perhaps due to its intrinsic property but not impurities. The E_{bd} is roughly twice that of H_2O-based film (deposited at 33 °C). The low breakdown field of H_2O-based Al_2O_3 film may result from the 22% hydrogen impurities in the Al_2O_3 films [16].

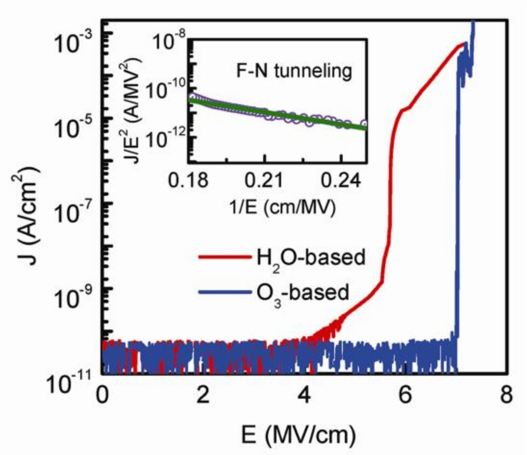

Fig. 5. The J-E plots of H_2O-based and O_3-based Al_2O_3 films, which are deposited at 300 ^oC and room temperature, respectively. The inset indicates the ln(J/E^2)-1/E plot of the H_2O-based film.

4. Conclusions

In conclusion, the high quality Al_2O_3 films were prepared via ALD process without any assistance at room temperature. TMA and ozone were used as Al and O source, respectively. The deposition velocity almost improved two orders of magnitude with the using of O_3 instead of H_2O. It has been found that the O_3-based Al_2O_3 film has much low defects density and excellent insulating performance compares to the H_2O-based Al_2O_3 film. The rather short purge time facilitates the improvement of throughout. The fabrication method without any heat process is helpful for the reduction of thermal consumption in manufacturing process and supplies the compatibility with kinds of flexible electronic devices, OLEDs, DSSCs, etc.

Acknowledgments

This work was financially supported by the National Natural Science Foundation of China (Grant Nos. 60906046, 60990312, 61106122 and 11074076), the State Key Basic Research Program of China (Grant No. 2011CB922200), Projects of Science and Technology Commission of Shanghai Municipality (Grant Nos. 10DJ1400200, 10ZR1409800, 09ZZ42, 10SG28, and 11520701300), the Innovation Research Project of East China Normal University, the Program for Professor of Special Appointment (Eastern Scholar) at Shanghai Institutions of Higher Learning, and PCSIRT.

References

[1] H. C. Lin, P. D. Ye, G. D. Wilk, Appl. Phys. Lett. **87,** 182904 (2005).

[2] S. van Dijken, X. Jiang, S. S. P. Parkin, Appl. Phys. Lett. **80**, 3364 (2002).

[3] B. Díaz, E. Härkönen, J. Swiatowska, V. Maurice, A. Seyeux, P. Marcus, M. Ritala, Corros. Sci. **53**, 2168 (2011).

[4] Y. Xuan, H. Lin, P. Ye, G. Wilk, Appl. Phys. Lett. **88,** 263518 (2006).

[5] J. Meyer, D. Schneidenbach, T. Winkler, S. Hamwi, T. Weimann, P. Hinze, S. Ammermann, H. H. Johannes, T. Riedl, W. Kowalsky, Appl. Phys. Lett. **94,** 233305 (2009).

[6] M. Weaver, L. Michalski, K. Rajan, M. Rothman, J. Silvernail, J. J. Brown, P. E. Burrows, G. L. Graff, M. E. Gross, P. M. Martin, Appl. Phys. Lett. **81,** 2929 (2002).

[7] M. Law, L. E. Greene, A. Radenovic, T. Kuykendall, J. Liphardt, P. Yang, J. Phys. Chem. B **110**, 22652 (2006).

[8] J. Schmidt, A. Merkle, R. Brendel, B. Hoex, M. C. M. de Sanden, W. Kessels, Progress in Photovoltaics: Research and Applications **16,** 461 (2008).

[9] I. S. Jeon, J. Park, D. Eom, C. S. Hwang, H. J. Kim, C. J. Park, H. Y. Cho, J. H. Lee, N. I. Lee, H. K. Kang, Jpn. J. Appl. Phys **42,** 1222 (2003).

[10] W. S. Yang, Y. K. Kim, Y. Seung-Yeal, J. H. Choi, H. S. Park, S. I. Lee, Y. Ji-Beom, Surf. Coat. Technol. **131,** 79 (2000).

[11] S. J. Yun, H. R. Kim, K. S. Nam, K. H. Lee, J. Skarp, Flat panel display materials III **471**, 81 (1997).

[12] J. Klaus, S. George, J. Electrochem. Soc. **147**, 2658 (2000).

[13] S. E. Potts, W. Keuning, E. Langereis, G. Dingemans, M. C. M. van de Sanden, W. M. M. Kessels, J. Electrochem. Soc. **157**, 66 (2010).

[14] R. L. Puurunen, H. Kattelus, T. Suntola, Handbook of Silicon Based MEMS Materials and Technologies, William Andrew, Burlington, 2009, p.433.

[15] T. O. Kääriäinen, D. C. Cameron, Plasma Process. Polym. **6,** S237 (2009).

[16] M. D. Groner, F. H. Fabreguette, J. W. Elam, S. M. George, Chem. Mater. **16,** 639 (2004).

[17] T. Watanabe, H. H. Funke, R. Torres, M. W. Raynor, J. Vininski, V. H. Houlding, J. Cryst. Growth **248,** 67 (2003).

[18] R. L. Puurunen, J. Appl. Phys. **97,** 121301 (2005).

[19] T. Suntola, Appl. Surf. Sci. **100,** 391 (1996).

[20] P. Kirsch, M. Quevedo-Lopez, H. J. Li, Y. Senzaki, J. Peterson, S. Song, S. Krishnan, N. Moumen, J. Barnett, G. Bersuker, J. Appl. Phys. **99,** 023508 (2006).

[21] M. Rose, J. Niinistö, I. Endler, J. W. Bartha, P. Kücher, M. Ritala, ACS Appl. Mater. Interfaces **2,** 347 (2010).

[22] H. B. Park, M. Cho, J. Park, S. W. Lee, T. J. Park, C. S. Hwang, Electrochem. Solid-State Lett. **7,** G254 (2004).

[23] J. B. Kim, D. R. Kwon, K. Chakrabarti, C. Lee, K. Y. Oh, J. H. Lee, J. Appl. Phys. **92,** 6739 (2002).

[24] C.-W. Cheng, E. A. Fitzgerald, Appl. Phys. Lett. **93,** 031902 (2008).

[25] A. Ott, J. Klaus, J. Johnson, S. George, Thin Solid Films **292,** 135 (1997).

[26] T. Hori: Gate Dielectric, MOS ULSIs, Springer, Berlin, 1997, Chap. 2, p. 55.

[27] S. Lombardo, J. H. Stathis, B. P. Linder, K. L. Pey, F. Palumbo, C. H. Tung, J. Appl. Phys. **98,** 121301 (2005).

[28] M. D. Groner, J. W. Elam, F. H. Fabreguette, S. M. George, Thin Solid Films **413,** 186 (2002).

[29] C. H. Ko, W. J. Lee, J. Solid State Electrochem. **11,** 1391 (2007).

---

[*] Corresponding author: ywli@ee.ecnu.edu.cn